Assessment of Particle Drag Models Using GBK Experimental Data

Grant Palmer[1] and Amal Sahai[2]
AMA, Inc. at NASA Ames Research Center, Moffett Field, CA, 94035, United States

Dirk Allofs[3], Dominik Neeb[3], and Ali Guelhan[4]
German Aerospace Center (DLR), Cologne, Germany

Nomenclature

A = cross-sectional area, m^2
c = speed of sound, m/s
C_D = drag coefficient
d_p = particle diameter, m
F_D = drag force, N
Kn = Knudsen number
m = mass, kg
M = Mach number
Re = Reynolds number
$\vec{v}$ = velocity, m/s
μ = viscosity, kg/m-s
ρ = density, kg/m^3

Subscripts
g = gas
p = particle

I. Introduction

The analysis of dust-laden flows can be an important element of spacecraft design. For example, a spacecraft entering the Martian atmosphere will encounter dust particles suspended in the atmosphere. If the entry occurs during a major regional or global dust storm, dust particle impacts on the heatshield of the spacecraft can cause erosion of the vehicle thermal protection system (TPS) that can be equivalent to that caused by thermochemical ablation [1]. There is also a possibility of particulate matter in the atmosphere of Titan that may impact the Dragonfly project capsule during its atmospheric entry. Vehicles landing on the surface of Mars or on the Earth's moon may also liberate surface dust or regolith due to plume-surface interaction (PSI) effects [2].

Developing a simulation capability to model dust-laden flows requires the ability to accurately predict the velocity of a particle as it travels through a shock layer, nozzle plume, or the flow of an experimental facility. The primary mechanism that determines the particle velocity is the drag force acting on the particle. The drag force is typically expressed in terms of the frontal area of the particle, its velocity relative to the surrounding fluid, the density of the surrounding fluid, and a non-dimensional drag coefficient. Substantial effort has been devoted over many decades to developing models or correlations to estimate the drag coefficient for spherical bodies over a wide range of flow conditions [5] – [10]. The correlations have historically been based on experimental data, but more recently computational simulations have been used to augment the experimental data [5].

Since 2017 there has been a successful partnership between the NASA Entry Systems Modeling (ESM) project under the NASA Game Changing Development (GCD) program and the German Aerospace Center (DLR). Dusty flow experiments have been performed in the DLR GBK facility [3]. DLR has developed advanced diagnostic

[1] Research Scientist, Aerothermodynamics Branch, AIAA Associate Fellow.
[2] Research Scientist, Aerothermodynamics Branch, AIAA member
[3] Research Scientist, Department of Supersonic and Hypersonic Technologies
[4] Department Head, Department of Supersonic and Hypersonic Technologies

techniques in the GBK facility that allow simultaneous measurement of particle size, velocity, and mass flow rate [3]. This new high-precision experimental data is well-suited to drag model validation efforts

As part of the ESM project, an integrated CFD-particle trajectory code named US3D-DUST is being developed [4]. This code uses a Lagrangian-based framework that computes the trajectories of individual particles in the flow. Several of the most commonly-used spherical drag models have been implemented in US3D-DUST. In this study, the US3D-DUST code will be used to simulate particle flows in the GBK facility. Differences in particle velocities predicted using the different drag models will be compared against recent GBK data.

II. Characterizing Dusty Flow Environments

The dusty flow environment experienced by a particle traveling through a shock layer or the flow through an experimental facility can be characterized in terms of the particle Mach, Reynolds, and Knudsen numbers. These non-dimensional numbers are similar to the standard definitions applied to gas flows, with the difference being that the particle non-dimensional numbers are based on the relative particle velocity, $\Delta\vec{V}$, between the particle and the surrounding fluid.

$$\Delta\vec{V} = \overrightarrow{v_g} - \overrightarrow{v_p} \tag{1}$$

A. Reynolds Number

The particle Reynolds is a function of the relative particle velocity, the particle diameter, and the density and viscosity of the fluid surrounding the particle.

$$Re = \frac{\rho_g |\Delta\vec{V}| d_p}{\mu_g} \tag{2}$$

The particle Reynolds number determines the nature of the boundary layer flow around the particle. If the particle Reynolds number is much less than 1, the particle is in a flow condition known as the "creeping flow" regime [5]. Viscous effects dominate, and the flow is laminar and fully-attached over the entire sphere. This condition is also referred to as the Stokes drag regime. The boundary layer around the particle continues to be laminar and attached for particle Reynolds numbers less than 20. As Reynolds numbers continue to increase up to a value of about Re = 130, the wake flow behind the particle is separated but steady. At still higher Reynolds numbers, up to Re = 1500, the laminar wake becomes unsteady and transitional. For Reynolds numbers between 2000 and 2.0×10^5, a laminar boundary layer on the front of the sphere will separate at an angle of 80 degrees, and this flow separation creates a fully turbulent wake behind the particle. The drag coefficient in this region is more or less constant with a value between 0.4 and 0.45, a value known as the "critical drag coefficient". This constant drag coefficient behavior was noticed by Newton in 1710.

B. Mach Number

The particle Mach number characterizes the extent of compressibility effects on the flow around the particle and is equal to the magnitude of the relative particle velocity divided by the speed of sound in the fluid surrounding the particle.

$$M = \frac{|\Delta\vec{V}|}{c} \tag{3}$$

Because the particle Mach number is based on the relative particle velocity, a slow-moving particle striking a fast-moving shock layer (e.g., in front of a spacecraft) and a fast-moving particle striking a stationary shock wave (e.g., in front of a model in an arcjet experiment) can both experience supersonic particle Mach numbers

The flow is considered to be incompressible at particle Mach numbers less than about 0.1. Early spherical drag correlations, such as the Stokes equation [7], were based on incompressible, continuum flow. At particle Mach numbers between 0.1 and 0.65, the flow is still subsonic, but compressibility effects have increased to the point that they must be included in the drag model [6]. As the particle Mach number continues to increase, the flow regime will change from subsonic, to transonic, to supersonic conditions. At Mach numbers above 5, the flow is considered to be hypersonic. The Mach number primarily affects the particle drag coefficient in the compression-dominated drag regime, which occurs when the particle Reynolds number is greater than 45.

C. Knudsen Number

The particle Knudsen number is defined as the ratio of the mean free path of the fluid surrounding the particle to the particle diameter. The Knudsen number can be expressed in terms of the particle Mach and Reynolds numbers [5].

$$Kn = \sqrt{\frac{\pi\gamma}{2}}\left(\frac{M}{Re}\right) \tag{4}$$

The γ term in Eq. (4) is the specific heat ratio of the surrounding fluid. Since the Knudsen number is a function of the Mach and Reynolds numbers, the three quantities are not mutually independent. Specifying the values of two of them will define the third.

The are four general flow regimes defined in terms of the particle Knudsen number. The continuum flow regime is when the Knudsen number is less than 0.01 and indicates that the particle Reynolds number is larger than the particle Mach number by two orders of magnitude or more. The slip regime is defined by Knudsen numbers between 0.01 and 0.1. At higher Knudsen numbers between 0.1 and 10, the particle is in the transitional flow regime. Free molecular flow occurs when the Knudsen number is greater than 10. In the rarefaction-dominated regime where Re < 45, drag coefficient decreases with increasing Knudsen number, which intuitively makes sense because free-molecular conditions will offer less drag resistance than continuum flows.

D. General Trends in Drag Coefficient

The general trends of spherical drag coefficient with regards to Reynolds, Mach, and Knudsen number are shown in Fig. 1. As presented by Loth [6], the particle Reynolds number defines two distinct regions of spherical drag coefficients. There is a "nexus" condition at Re = 45 where drag coefficient is independent of both Mach and Knudsen number with a value of approximately 1.63. At Reynolds numbers less than 45, the particles are in the rarefaction-dominated regime where Knudsen number has a strong effect on the drag coefficient. In this regime, the upper-bound limiting curve is the Stokes curve that represents incompressible, continuum, low Reynolds number flow. The lower-bound limiting curve in the rarefaction-dominated regime is for free-molecular flow where the drag coefficient has a value of around 2 at low Reynolds numbers and decreases slightly as Reynolds number increases.

At Reynolds numbers larger than 45, the particles are in the compression-dominated regime where the drag coefficient is primarily influenced by compressibility (i.e., Mach number) effects. The lower-bound curve in the compression-dominated regime is for incompressible, low Mach number flow where the drag coefficient value reaches the "critical drag coefficient" value of 0.42 – 0.45. The upper-bound limiting curve is for Mach >> 1.

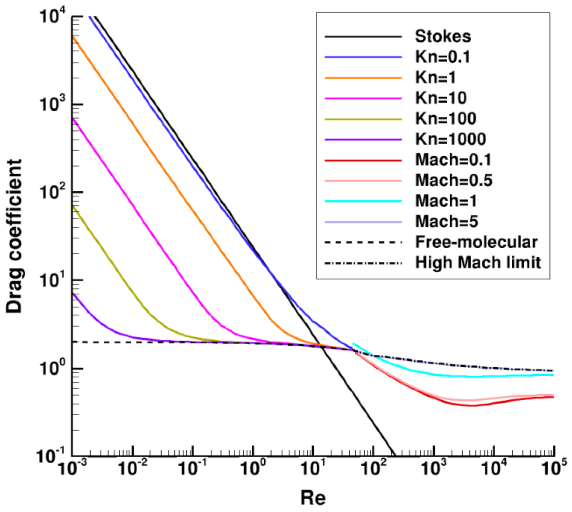

Figure 1. General trends of particle drag coefficient.

III. Drag Correlations for Incompressible Continuum Flow

The quasi-steady drag force on a spherical particle can be expressed in terms of the relative particle velocity, the diameter of the particle, the density of the surrounding fluid, and a non-dimensional drag coefficient.

$$\overrightarrow{F_D} = m_p \frac{d\overrightarrow{V_p}}{dt} = \frac{1}{2}\rho_g \cdot \left|\Delta \vec{V}\right|\Delta\vec{V} \cdot C_D A = \frac{1}{8}\pi d_p^2 \rho_g \cdot \left|\Delta \vec{V}\right|\Delta\vec{V} \cdot C_D \tag{5}$$

One of the earliest sphere drag correlations was developed by Stokes [7] for incompressible continuum flows with $Re \ll 1$. According to the Stokes derivation, the drag coefficient of the sphere is linear with the inverse of particle Reynolds number.

$$C_D = \frac{24}{Re} \tag{6}$$

To extend the Stokes correlation for higher Reynolds numbers, Clift and Gauvin [9] developed a correlation that multiplies the Stokes equation by a correction factor and adds a second term that transitions to what is called the critical drag coefficient of 0.42 at Reynolds numbers above 2000.

$$C_D = \frac{24}{Re}(1 + 0.15Re^{0.687}) + \frac{0.42}{1+(42500/Re^{1.16})} \tag{7}$$

The left-hand term of Eq. (8), consisting of the Stokes correlation and correction factor is known as the Schiller-Naumann drag correlation [10] and can be used by itself for particle Reynolds numbers less than 800.

IV. Henderson Drag Model

The Stokes and Clift-Gauvin drag correlations are intended for spherical particles traveling through incompressible continuum flows. A more ambitious drag model for spheres was developed by Henderson [8]. Until recently, the Henderson model was the most commonly used, and considered the most accurate, sphere drag model for particle trajectory analysis. The model provides two equations that are applicable for subsonic and supersonic flows in continuum, slip, transitional, and free-molecular flow regimes.

The Henderson model equations are primarily designed to match the experimental data of Bailey and Hiatt [11] where spheres made from various materials ranging in size from 2.38 – 25.4 mm were fired in a ballistic range at Mach numbers ranging from 0.13 to 7. The particle Reynolds numbers in the test shots varied from 4.9 – 77.4x10^3. The resulting Henderson correlations are intended for particle Mach numbers up to 6 and Reynolds numbers up to the laminar-turbulent transition, which Loth [5] estimates occurs at around Re=1500. The Henderson model accounts for temperature differences between the surface of the particle and the surrounding fluid.

The Henderson drag coefficient equation for subsonic flow is a function of the particle Mach, Reynolds, and Knudsen numbers and the particle and fluid temperatures.

$$C_D = 24\left[Re + S\left\{4.33 + \left(\frac{3.65-1.53\frac{T_p}{T_g}}{1+0.353\frac{T_p}{T_g}}\right)exp\left(-0.247\frac{Re}{S}\right)\right\}\right]^{-1} + exp\left(-0.5\frac{M}{\sqrt{Re}}\right)\left[\frac{4.5+0.38\left(0.03Re+0.48\sqrt{Re}\right)}{1+0.03Re+0.48\sqrt{Re}} + 0.1M^2 + 0.2M^8\right] + 0.6S\left[1 - exp\left(-\frac{M}{Re}\right)\right] \tag{8}$$

The molecular speed ratio, S, is a function of particle Mach number, M, and is defined as:

$$S = M\sqrt{\frac{\gamma}{2}} \tag{9}$$

For supersonic Mach numbers greater than 1.75, the Henderson model uses the following expression:

$$C_D = 0.9 + \frac{0.34}{M^2} + 1.86\sqrt{\frac{M}{Re}}\left[2 + \frac{2}{S^2} + \frac{1.058}{S}\sqrt{\frac{T_p}{T_g}} - \frac{1}{S^4}\right]\Big/\left(1 + 1.86\sqrt{\frac{M}{Re}}\right) \tag{10}$$

One weakness of the Henderson correlation is that there is a gap between the subsonic correlation that goes up to Mach = 1 and the supersonic correlation that starts at a Mach number of 1.75. Henderson recommended a linear interpolation between the drag coefficients at Mach 1 and 1.75. Another deficiency of the Henderson model is that it is largely based on the data from Ref. [11], but most of that experimental data was taken in the continuum and slip flow regimes. There are only 9 cases that were run in transitional flow conditions, and all of them were run at the low end of that regime with a maximum Knudsen number value of 0.138. Therefore, very little experimental data is used to anchor the Henderson model in the transitional flow regime which is the relevant condition for dust particles traveling through Martian shock layers.

V. Loth Drag Model

In 2008, Loth [6] presented a new spherical drag model that consisted of separate correlations for the rarefaction- and compression-dominated regimes. In addition to the Bailey and Hiatt data, the Loth correlations were also based on additional ballistic range experimental data including that of Hoerner [12]. In 2021, Loth, et al. [5] updated the 2008 drag model with additional experimental data as well as DSMC simulations that were used to provide data at lower particle Reynolds numbers in the slip and transitional flow regimes.

A. Drag Coefficient in the Rarefaction-Dominated Regime

The Loth 2021 drag model consists of two sets of correlations for the rarefaction- and compression-dominated regimes. In the rarefaction-dominated regime there are two limiting cases for drag coefficient. The upper bound of drag coefficient values is the incompressible continuum limit for Reynolds numbers much less than one, i.e., the Stokes curve, where the Knudsen number approaches zero. For low Mach number flows with non-zero Knudsen numbers, the drag coefficient in the rarefied-dominated regime can be expressed as the Schiller-Naumann component of the Clift-Gauvin correlation multiplied by a correction factor that accounts for Knudsen number effects [5].

$$C_{D,Kn,Re} = \frac{24}{Re}(1 + 0.15Re^{0.687}) \frac{1}{1+Kn\left[2.514+0.8\exp\left(-\frac{0.55}{Kn}\right)\right]} \tag{11}$$

Equations (11) is intended for low particle Mach numbers where compressibility effects are minimal. The other limiting case in the rarefaction-dominated regime is for free-molecular flow, where it is assumed that the particle Mach and Knudsen numbers are high [5]. The correlation for free molecular flow is a function of the molecular speed ratio defined in Eq. (9) and the error function.

$$C_{D,fm} = \frac{\left(1+2S^2\right)exp\left(-S^2\right)}{S^3\sqrt{\pi}} + \frac{\left(4S^4+4S^2-1\right)\mathrm{erf}\left(S\right)}{2S^4} + \frac{2}{3S}\sqrt{\pi} \tag{12}$$

When the molecular speed ratio, and therefore particle Mach number, become very large, the value of $C_{D,fm}$ approaches 2, which is the lower limit of drag coefficient in rarefied flow for low Reynolds numbers. For larger Reynolds numbers, the free-molecular drag coefficient is modified using an empirical scaling factor.

$$C_{D,fm,Re} = \frac{C_{D,fm}}{1+\left[\left(C_{D,fm}/J_M\right)-1\right]\sqrt{Re/45}} \tag{13}$$

The expressions for the coefficient, J_M, are functions of particle Mach number and can be found in Ref. [5]. To determine the overall drag coefficient in the rarefaction-dominated regime, the low- and high-Mach number expressions are blended using the particle Mach number.

$$C_D = \frac{C_{D,Kn,Re}}{1+M^4} + \frac{M^4 C_{D,fm,Re}}{1+M^4} \tag{14}$$

B. Drag Coefficient in the Compression-Dominated Regime

In the compression-dominated regime when Re > 45, the spherical drag coefficient for incompressible, continuum flow coefficient decreases gradually before reaching the critical drag coefficient value of about 0.42 for Reynolds

numbers less than 2.0×10^5. The drag coefficient for incompressible, continuum flow can be estimated using the Clift-Gauvin correlation shown in Eq. (7). It is well-known that increasing Mach number in the compression-dominated regime will increase drag coefficient [5]. To account for Mach number effects, Loth, et al. [5] propose a modified Clift-Gauvin expression that shows a good match to the available experimental and simulation data over a Mach number range from 0.25 to 10.

$$C_D = \frac{24}{Re}(1 + 0.15Re^{0.687})H_M + \frac{0.42C_M}{1+\left({}^{42500}/_{Re^{1.16C_M}}\right)+\left({}^{G_M}/_{Re^{0.5}}\right)} \tag{15}$$

The equations for the coefficients, C_M, G_M, and H_M, are functions of particle Mach number and can be found in Ref. [5]. A limiting case for the Loth drag correlation in the compression-dominated regime is for high Mach numbers where $M \gg 1$. In this situation, the coefficients shown in Eq. (15) reduce to single values.

$$C_D = \frac{22.32}{Re}(1 + 0.15Re^{0.687}) + \frac{0.861}{1+\left({}^{42500}/_{Re^{2.38}}\right)+\left({}^{5}/_{Re^{0.5}}\right)} \tag{16}$$

VI. The US3D-DUST Code

The US3D code is a Navier-Stokes flow solver that was developed at the University of Minnesota in collaboration with the NASA Ames Research Center for the simulation of compressible and reacting flows [13]. The US3D code has been applied to a wide range of aeronautical and aerothermal flow problems and is one of the main CFD codes used by the NASA Entry, Descent, and Landing (EDL) community. Recently as part of the ESM project, a Lagrangian particle solver named DUst Simulation and Tracking (DUST) [4] has been integrated into the US3D flow code.

The DUST solver provides a time-varying solution for particle attributes such as location, velocity, temperature, and diameter using the point-particle discrete element method. Inter-phase and intra-phase interactions, characterized as one, two, or four way coupling between carrier and dispersed phase, can be modeled to varying levels of completeness based on problem requirements within the same framework. A central component of this solver is the particle mesh-location algorithm which utilizes standard unstructured mesh connectivity information to efficiently identify the sequence of Eulerian cells a particle traverses through during the simulation. This also streamlines subsequent operations related to enforcing boundary conditions, parallelization over a distributed memory system, and determining the coupling source terms for the surrounding flow. The time-driven hard-sphere approach is adopted to speed up calculations for resolving particle-particle collisions. Time-stepping is performed using Adams-Bashforth methods which balances temporal accuracy and computational costs.

The DUST library in conjunction with US3D has been applied to study a range of problems. These include verification tests involving hypersonic planetary entry, flow through a converging-diverging nozzle, and the impingement of dust particles on a flat plate. Additionally, surface heat-flux augmentation due to particle impacts has been numerically investigated for the Mars 2020 spacecraft during its descent through the dusty Martian atmosphere.

VII. The GBK Facility

The multi-phase flow facility (GBK) is a small test facility that is part of the German Aerospace Center (DLR) supersonic wind tunnel complex [3]. The GBK is a blow down facility that injects high-pressure air from reservoir tanks to generate a Mach 2.1 flow condition at the exit plane of a de Laval nozzle. The test gas is air and includes a heated main flow and an unheated "bypass" flow. Particles can be injected through the bypass tube into the test gas. The maximum design air pressure is 5.4 MPa, and the maximum total air flow rate is about 1.5 kg/s [3]. An instrumented probe, typically of hemispherical shape, can be placed at a distance downstream of the nozzle exit.

Recent improvements to the GBK have enhanced the non-intrusive measurement capabilities of the facility [3]. Simultaneous particle size and velocity measurements can be obtained using a shadowgraphy system. Measurements of the particle-laden flow can also be taken with a Particle Image Velocimetry (PIV) system. The minimum detectable size for the shadography was determined to be between 10 and 20 microns. The averge uncertainty of the particle size measurements was estimated to be 2.5 microns. The velocity uncertainty decreased with increasing particle velocity generally ranging from 5 – 15%.

Most of the tests considered in this paper used Al_2O_3 particles with a diameter greater than 15 microns, which could be more readily be detected by the shadowgraphy [3]. The density of Al_2O_3 was assumed to be 3950 kg/m^3. One

test was performed with MgO particles with a smaller size of about 0.2 microns. A 12 mm diameter hemisphereical model was located 5 mm downstream of the nozzle exit. The shadowgraphy data was taken at an average location of 2.5 mm downstream of the nozzle exit close to the bow shock wave that forms in front of the model. The stagnation pressure and temperature in the GBK chamber were 0.949 MPa and 373.1 K. The main air flow rate was 0.718 kg/s and the bypass flow rate was 0.045 kg/s.

VIII. Results

Particle trajectories were computed in the GBK nozzle flow using US3D-DUST for a 0.2 micron diameter MgO particle as well as for Al_2O_3 particles ranging in size from 15 to 70 microns. The simulations were performed using one-way fluid-particle coupling where the fluid altered the particle velocity, but the particles had no impact on the surrounding fluid. The US3D-DUST simulations were peformed using four different spherical drag models. The Clift-Gauvin correlation shown in Eq. (7) represents the incompressible, continuum limit. The Henderson and Loth 2021 drag models were also used in the simulations. The fourth drag model used was the Loth 2021 model in the high Mach number limit shown in Eq. (16). The Clift-Gauvin and high Mach number curves represent the upper and lower bounds of experimental and theoretical spherical drag coefficient values in the compression-dominated regime.

The interaction of the fluid and particles dependes on the location of the particle in the GBK flow. Upstream of the converging section of the nozzle, the flow velocity is relatively low, around 25 m/s. The length of the chamber is sufficient that at the start of the converging section of the nozzle the particle velocity is essentially the same as that of the surrounding fluid. The fluid accelerates as it travels through the converging and diverging sections of the nozzle. The particle velocity will lag that of the surrounding flow. Since the fluid is traveling faster than the particle, the drag forces on the particle will pull the particle forward increasing the particle velocity. Larger, heavier particles will accelerate more slowly than smaller, lighter particles, so when the particles exit the nozzle the velocity of the larger particles will be less than that of smaller particles.

The flow regimes experienced by the Al_2O_3 particles were extracted from the US3D-DUST simulations. The particle Reynolds number for a 15-micron particle is about 175 when the flow begins to accelerate in the converging section of the nozzle, increases to 580 – 590 at the nozzle throat, and then decreases to 320 at the nozzle exit. The larger diameter particles experience higher Reynolds numbers, so all of the Al_2O_3 particles were in the compression-dominated drag coefficient regime. The Knudsen numbers for all of the Al_2O_3 particle sizes were less than 0.001 throughout the GBK flow, so the Al_2O_3 particles were in the continuum flow. The particle Mach numbers in the areas of interest are largely subsonic with the larger particles entering the transonic regime downstream of the nozzle exit. There is one experimental data point for a 0.2-micron MgO particle, but these particles were small enough that they quickly equilibrated with the flow velocity and therefore are of less interest when evaluating particle drag models.

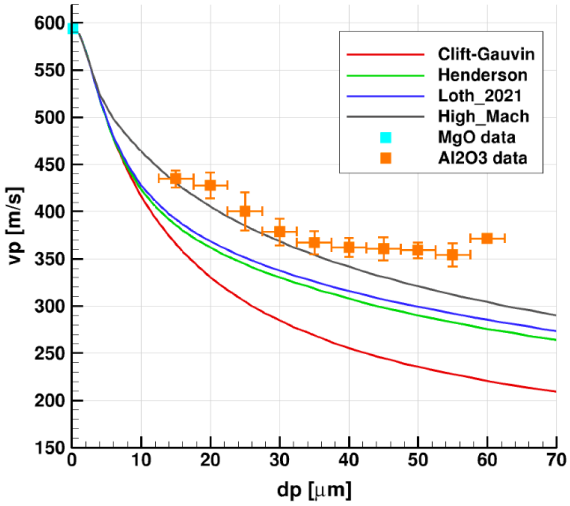

Fig. 4. Experimental and computational particle velocities, 2.5 mm downstream of nozzle exit.

The experimental and computational values of particle velocity 2.5 mm downstream of the nozzle exit as a function of particle diameter are shown in Fig. 4. For particle diameters between 15- and 40-microns, the measured particle

velocities follow the expected behavior in that particle velocity decreases as particle size increases. The experimental velocities are higher than the high Mach curve, which theoretically should be the upper bound of spherical particle drag. For particle sizes greater than 40-microns, the particle velocities do not decrease with increasing particle size but instead level out to a more or less constant value increasingly deviating from the high Mach number curve. The Loth 2021 spherical drag model, which claims to be more accurate than the older Henderson drag model, predicts slightly higher velocities than the Henderson values and therefore is slightly closer to the experimental values.

There are several possible reasons that the measured particle velocities are outside of the theoretical range defined by the high Mach number curve. Higher experimental particle velocities indicate that the particles experienced a higher drag force than predicted by the spherical drag models. One possible reason for this discussed by Allofs, et al. [3] is that the particles may not have been spherical. A non-spherical particle may have a larger average frontal area than the spherical value of πr^2. Allofs, et al. [3] speculated that agglomeration of the particles into larger, non-spherical shapes may have reduced the effective particle density of the Al_2O3 particles below the pure substance density of 3950 kg/m^3. As reported in Ref. [3], there is ongoing research at DLR to reduce the uncertainties in both the particle velocity and size measurements in the GBK experiments.

IX. Concluding Remarks

The integrated CFD-particle trajectory code, US3D-DUST, was used to simulate dusty-flow conditions in the DLR GBK facility. Four different spherical particle drag models were used to estimate particle velocities as a function of particle size at a location 2.5 mm downstream of the GBK exit plane where simultaneous measurements of particle size and velocity were taken using advanced shadowgraphy techniques. The measured particle velocities were larger than all of the simulation profiles, even the theoretical high Mach number limit indicating that the particles in the experiment experienced a higher drag force than predicted by the spherical drag models. One possible reason for the discrepancy was that the particles may have been non-spherical. Additional experiments should be performed in the GBK using new techniques to reduce the uncertainty in the particle velocity and size measurements. The ultimate goal of this research may be to develop a new drag model for non-spherical particles.

References

[1] Palmer, G., Ching, E., Ihme, M., Allofs, D., and Gülhan, A., "Modeling Heatshield Erosion due to Dust Particle Impacts for Martian Entries," *Journal of Spacecraft and Rockets*, Vol. 57, No. 5, 2020, pp. 857-875.

[2] Patel, M., Rabinovitch, J., Capcelatro, J., "Eulerian-Lagrangian simulations of plume-induced sheared granular beds under Martian conditions," AIAA Paper 2022-2193, Jan. 2022.

[3] Allofs, D., Neeb, D., and Guelhan, A., "Simultaneous determination of particle size, velocity, and mass flow in dust-laden supersonic flows," Experiments in Fluids (2022), 63:86, https://doi.org/10.1007/s00348-022-03402-z.

[4] Sahai, A. and Palmer, G. "A Variable Fidelity Euler-Lagrange Framework for Simulating Particle-Laden High-Speed Flows," *AIAA Journal*, Accepted for publication October 2021.

[5] Loth, E., "Supersonic and Hypersonic Drag Coefficients for a Sphere", *AIAA Journal*, Vol. 59, No. 8, 2021, pp. 3261-3274.

[6] Loth, E., "Compressibility and Rarefaction Effects on Drag of a Spherical Particle", *AIAA Journal*, Vol. 46, No. 9, 2008, pp. 2219-2228.

[7] Stokes, G. G., "On the Effect of the Internal Friction of Fluids on the Motion Of Pendulums," Transactions of the Cambridge Philosophical Society (Mathematical and Physical Sciences), Vol. 9, Pt. 2, 1851, pp. 8–106.

[8] Henderson, C.B., "Drag Coefficients of Spheres in Continuum and Rarefield Flows," *AIAA Journal*, Vol. 14, No. 6, 1976, pp. 707-718.

[9] Clift, R., and Gauvin, W. H., Proceedings of CHEMECA '70, Vol. 1, Butterworth, Melbourne, 1970, pp. 14–28.

[10] Schiller, L., and Naumann, A. Z., "Über die Grundlegenden Berechungen bei der Schwerkraftaufbereitung," Zeitschrift des Vereines Deutscher Ingenieure, Vol. 77, No. 12, 1933, pp. 318–320.

[11] Bailey, A.B. and Hiatt, J., "Free-Flight Measurements of Sphere Drag at Subsonic, Transonic, Supersonic, and Hypersonic Speeds for Continuum, Transition, and Near-Free-Molecular Flow Conditions," AEDC-TR-70-291, 1971.

[12] Hoerner, S. F., Fluid-Dynamic Drag, published by Hoerner, S. F., Midland Park, NJ, 1958.

[13] Candler, G.V., Johnson, H.B., Nompelis, I., Gidzak, V.M., Subbareddy, P.K., and Barnhardt, M., "Development of the US3D code for advanced compressible and reacting flow simulations," AIAA Paper 2015-1893, Jan. 2015.